Research Paper
Computational Methods for Differential Equations
http://cmde.tabrizu.ac.ir
Vol. 14, No. 1, 2026, pp. 188-200
DOI:10.22034/cmde.2025.65052.2970

Numerical simulation of a nonlinear system of space-fractional Klein-Gordon-Zakharov equations using the Fourier spectral method

Zohreh Yaghoobloo[1], Sedigheh Toubaei[1,*], Mehdi Jalalvand[2], Jafar Esmaily[1], and Safiyeh Mohammadian[3]

[1]Department of Mathematics, Ahvaz branch, Islamic Azad University, Ahvaz, Iran.

[2]Department of Mathematics, Faculty of Mathematical Sciences and Computer, Shahid Chamran University of Ahvaz, Ahvaz, Iran.

[3]Department of Mathematics, Osku Branch, Islamic Azad University, Osku, Iran.

Abstract

An accurate and efficient numerical approach for the nonlinear space-fractional Klein-Gordon-Zakharov (KGZ) system of equations incorporating the fractional Laplacian operator is proposed in this study. The method is designed to preserve both mass and energy, which is crucial for accurately solving such complex systems. The spatial discretization is carried out using the Fourier spectral method. In contrast, temporal discretization is achieved through the fourth-order exponential time-differencing Runge-Kutta (ETDRK4) technique, ensuring both efficiency and stability. We prove the convergence of the proposed method, establishing a theoretical foundation for its application. To assess the efficiency and versatility of the proposed method, we report on a series of numerical simulations. The outcomes of these simulations are displayed in tables and graphs, illustrating the performance of the method regarding the approximation error, convergence order, and execution time for various fractional values.

Keywords. Nonlinear Klein-Gordon-Zakharov system, Space-fractional system, Laplacian operator of the fractional order, Fourier spectral method, Exponential Runge-Kutta of the fourth-order.

2010 Mathematics Subject Classification. 65N35, 26A33, 35Q53.

1. Introduction

The Zakharov equations, introduced by V.E. Zakharov, are among the most prominent partial differential equations in plasma physics, particularly in the study of Langmuir wave propagation. Zakharov's groundbreaking work demonstrated that Langmuir turbulence in plasma becomes unstable when it reaches a certain intensity, leading to the formation of low-density regions called "caverns," which serve as mechanisms for energy dissipation in long-wavelength Langmuir oscillations. Due to the accuracy of the Zakharov system in describing the coupling between high-frequency Langmuir waves and low-frequency ion-acoustic waves, it has also found applications in various physical phenomena, including shallow water waves and nonlinear optics [16, 20].

From a mathematical perspective, the Zakharov equations have been extensively studied, with research focusing on the existence and uniqueness of different solutions, such as small amplitude and global smooth solutions. Further, fractional extensions of these equations have been developed, offering deeper insights into their dynamics, both mathematically and numerically. These fractional systems retain energy-like conserved quantities, which have motivated the development of energy-preserving numerical methods. Despite these advancements, research on energy-conserving schemes remains limited, particularly in the fractional case. Key studies have also examined the well-posedness and suitable conditions for Zakharov-Kuznetsov systems and related models, further cementing the significance of Zakharov-type equations in the analysis of nonlinear systems and partial differential equations [8, 13, 14].

Received: 16 December 2024; Accepted: 03 March 2025.
∗ Corresponding author. Email: stoobaei@yahoo.com.

In this paper, we consider the double-fractional Klein-Gordon-Zakharov (KGZ) system

$$\begin{cases} \frac{\partial^2 \mathcal{V}}{\partial t^2} - \frac{\partial^\gamma \mathcal{V}}{\partial |x|^\gamma} + \mathcal{V} + \mathcal{W}\mathcal{V} + |\mathcal{V}|^2\mathcal{V} + \Phi(x,t) = 0, & (x,t) \in \mathbb{R} \times (0,t_f], t_f > 0, \\ \frac{\partial^2 \mathcal{W}}{\partial t^2} - \frac{\partial^\Lambda \mathcal{W}}{\partial |x|^\Lambda} - \frac{\partial^\Lambda (|\mathcal{V}|^2)}{\partial |x|^\Lambda} + \Psi(x,t) = 0, & (x,t) \in \mathbb{R} \times (0,t_f], t_f > 0, \\ \mathcal{V}(x,t) = \mathcal{V}(x+2\pi,t), \ x \in \mathbb{R}, \ t \in (0,t_f], \\ \mathcal{W}(x,t) = \mathcal{W}(x+2\pi,t), \ x \in \mathbb{R}, \ t \in (0,t_f]. \end{cases} \tag{1.1}$$

The regarded initial conditions are as follows:

$$\begin{aligned} &\mathcal{V}(x,t) = \mathcal{V}(x+2\pi,t) = h_0(x), && \mathcal{V}_t(x,t) = \mathcal{V}_t(x+2\pi,t) = h_1(x), && t = 0, x \in \mathbb{R}, \\ &\mathcal{W}(x,t) = \mathcal{W}(x+2\pi,t) = g_0(x), && \mathcal{W}_t(x,t) = \mathcal{W}_t(x+2\pi,t) = g_1(x), && t = 0, x \in \mathbb{R}. \end{aligned}$$

Here, the space-fractional derivatives $\frac{\partial^\gamma \mathcal{V}}{\partial |x|^\gamma}$, $(1 < \gamma \leq 2)$ and $\frac{\partial^\Lambda \mathcal{W}}{\partial |x|^\Lambda}$, $(1 < \Lambda \leq 2)$ denote the Riesz fractional derivatives of order γ and Λ defined as [12, 18]:

$$\frac{\partial^\gamma \mathcal{V}}{\partial |x|^\gamma} = -0.5 \sec(0.5\pi\gamma)({}_a^{RL}\mathcal{D}_x^\gamma \mathcal{V} + {}_x^{RL}\mathcal{D}_b^\gamma \mathcal{V}),$$

and

$$\frac{\partial^\Lambda \mathcal{W}}{\partial |x|^\Lambda} = -0.5 \sec(0.5\pi\Lambda)({}_a^{RL}\mathcal{D}_x^\Lambda \mathcal{W} + {}_x^{RL}\mathcal{D}_b^\Lambda \mathcal{W}),$$

in which

$${}_a^{RL}\mathcal{D}_x^\gamma \mathcal{V} = \frac{1}{\Gamma(2-\gamma)} \partial_{x^2}^2 \int_a^x (x-r)^{1-\gamma} \mathcal{V}(r,t) dr,$$

$${}_x^{RL}\mathcal{D}_b^\gamma \mathcal{V} = \frac{1}{\Gamma(2-\gamma)} \partial_{x^2}^2 \int_x^b (x-r)^{1-\gamma} \mathcal{V}(r,t) dr,$$

and

$${}_a^{RL}\mathcal{D}_x^\Lambda \mathcal{W} = \frac{1}{\Gamma(2-\Lambda)} \partial_{x^2}^2 \int_b^x (x-r)^{1-\Lambda} \mathcal{W}(r,t) dr,$$

$${}_x^{RL}\mathcal{D}_b^\Lambda \mathcal{W} = \frac{1}{\Gamma(2-\Lambda)} \partial_{x^2}^2 \int_x^b (x-r)^{1-\Lambda} \mathcal{W}(r,t) dr.$$

Recently, there has been a growing interest in space fractional KGZ systems, which serve as the fractional counterparts of classical KGZ systems and account for long-range interactions. The authors of [4] introduce a numerically efficient model to approximate solutions of the fractional KGZ system, incorporating Riesz-type fractional derivatives. This model is specifically designed to preserve energy and employs fractional-order-centered differences for spatial discretization. They prove the existence, uniqueness, stability, and convergence of the solutions. In [17], the authors focus on a fractional version of the KGZ equation using the beta-derivative, deriving new solitary wave solutions by applying the fractional rational sinh-cosh method and the fractional *sech* method. In [19], the authors propose an efficient linearly implicit conservative difference solver for the fractional KGZ system. They first derive the system's energy conservation property in a discrete setting. Using mathematical induction, they demonstrate that the scheme is uniquely solvable.

Additionally, they show, through the discrete energy method and a "cut-off" function technique, that the solver achieves specific convergence rates in L_∞- and L_2-norms, and is unconditionally stable. In [9], Macías-Díaz assumes the existence of solutions for a finite-difference model of the fractional KGZ equation; however, this assumption has been proven to be non-trivial. In [10], the authors investigate a KGZ system involving spatial fractional derivatives. They propose a finite-difference scheme in the explicit form to obtain the approximation, which preserves the system's energy and maintains nonnegative energy quantities under flexible parameter conditions. The authors rigorously establish the scheme's boundedness, consistency, stability, and convergence.

This paper presents an efficient and conservative method for solving the double-fractional KGZ system by combining the Fourier spectral method for space discretization and the exponential time-differencing Runge-Kutta method of

the fourth-order (ETDRK4) for time discretization. We illustrate the effectiveness of this approach for tackling the system under periodic boundary conditions, where the fractional Laplacians of different orders are discretized using the Fourier spectral method. The remainder of this paper is organized as follows: Section 2 introduces a numerical method for solving the double-fractional KGZ system using the Fourier spectral and ETDRK4 methods. In section 3, we present numerical results for test examples to validate the theoretical results. Section 4 offers concluding remarks summarizing the key findings and implications of this research.

2. Numerical method

For $s \in \mathbb{N}$ and even $\mathcal{Z}$, define $\tau_k = k\delta t$ for $k = 1 : s$, and $x_i = a + i\mathfrak{H}$ for $i = 0 : \mathcal{Z}$. Let $\delta t = \frac{t_f}{s}$ be the step size in time direction and $\mathfrak{H} = \frac{b-a}{\mathcal{Z}}$ be the step size in space direction. To address the KGZ system (1.1), we utilize a truncation of the Fourier series defined as $\Pi_{\mathcal{Z}}(\mathcal{V}) := \sum_{k=-\mathcal{Z}}^{\mathcal{Z}} \hat{\mathcal{V}}_k e^{ikx}$, which converges uniformly to $\mathcal{V}$. Let

$$\hat{\mathcal{V}}_k = \frac{1}{2\pi} \int_0^{2\pi} \mathcal{V}(x) e^{-ikx} dx. \tag{2.1}$$

The discrete Fourier transform(FT) is defined as follows [15]:

$$\tilde{\mathcal{V}}_k := \frac{1}{\mathcal{Z} b_k} \sum_{j=0}^{\mathcal{Z}-1} \mathcal{V}_j \mathrm{e}^{-ikx_j}, \ k = -\frac{\mathcal{Z}}{2}, ..., \frac{\mathcal{Z}}{2},$$

where k represents the Fourier wave number, with $b_k = 1$ for $|k| < \frac{\mathcal{Z}}{2}$ and $b_k = 2$ for $|k| = \frac{\mathcal{Z}}{2}$. The inverse discrete FT is expressed as:

$$\mathcal{V}_j := \sum_{k=-\frac{\mathcal{Z}}{2}}^{\frac{\mathcal{Z}}{2}} \tilde{\mathcal{V}}_k \mathrm{e}^{ikx_j}, \ j = 0, 1, ..., \mathcal{Z} - 1.$$

Additionally, the operator $\frac{\partial^\gamma \mathcal{V}}{\partial |x|^\gamma}$ can be defined as [7]:

$$\frac{\partial^\gamma \mathcal{V}}{\partial |x|^\gamma} = - \sum_{k=-\frac{\mathcal{Z}}{2}}^{\frac{\mathcal{Z}}{2}} |k|^\gamma \tilde{\mathcal{V}}_k \mathrm{e}^{ikx_j}, \ j = 0, 1, ..., \mathcal{Z} - 1.$$

Consider the space defined as $\mathcal{P}_{\mathcal{Z}} := \mathrm{span}\{\mathrm{e}^{ikx} : -\mathcal{Z} \le k \le \mathcal{Z}\}$, and let $\mathcal{P} = \lim_{\mathcal{Z}\to\infty} \mathcal{P}_{\mathcal{Z}}$. The inner product in the discrete form is defined by

$$\langle \mathcal{V}, U \rangle = \frac{1}{\mathcal{Z}} \sum_{j=0}^{\mathcal{Z}-1} \mathcal{V}(x_j, t) \bar{U}(x_j, t).$$

To obtain a function $\mathcal{V} \in \mathcal{P}$ that satisfies the weak formulation of (1.1), the following system must hold for all $\Upsilon \in \mathcal{P}$:

$$\begin{cases} \langle \frac{\partial^2 \mathcal{V}(x,t)}{\partial t^2}, \Upsilon \rangle - \langle \frac{\partial^\gamma \mathcal{V}(x,t)}{\partial |x|^\gamma}, \Upsilon \rangle + \langle \mathcal{V}(x,t), \Upsilon \rangle + \langle \mathcal{V}(x,t) \mathcal{W}(x,t), \Upsilon \rangle + \langle |\mathcal{V}(x,t)|^2 \mathcal{V}(x,t), \Upsilon \rangle + \langle \Phi(x,t), \Upsilon \rangle = 0, \\ \langle \frac{\partial^2 \mathcal{W}(x,t)}{\partial t^2}, \Upsilon \rangle - \langle \frac{\partial^\gamma \mathcal{V}(x,t)}{\partial |x|^\gamma}, \Upsilon \rangle - \langle \frac{\partial^\gamma |\mathcal{V}(x,t)|^2}{\partial |x|^\gamma}, \Upsilon \rangle + \langle \Psi(x,t), \Upsilon \rangle = 0. \end{cases} \tag{2.2}$$

We seek $\mathcal{V}_{\mathcal{Z}}, \mathcal{W}_{\mathcal{Z}} \in \mathcal{P}_{\mathcal{Z}}$ such that for every $\Upsilon \in \mathcal{P}_{\mathcal{Z}}$, the following condition is satisfied:

$$\begin{cases} \langle \frac{\partial^2 \mathcal{V}_{\mathcal{Z}}(x,t)}{\partial t^2}, \Upsilon \rangle - \langle \frac{\partial^\gamma \mathcal{V}_{\mathcal{Z}}(x,t)}{\partial |x|^\gamma}, \Upsilon \rangle + \langle \mathcal{V}_{\mathcal{Z}}(x,t), \Upsilon \rangle + \langle \mathcal{V}_{\mathcal{Z}}(x,t) \mathcal{W}_{\mathcal{Z}}(x,t), \Upsilon \rangle + \langle |\mathcal{V}_{\mathcal{Z}}(x,t)|^2 \mathcal{V}_{\mathcal{Z}}(x,t), \Upsilon \rangle + \langle \Phi(x,t), \Upsilon \rangle = 0, \\ \langle \frac{\partial^2 \mathcal{W}_{\mathcal{Z}}(x,t)}{\partial t^2}, \Upsilon \rangle - \langle \frac{\partial^\gamma \mathcal{V}_{\mathcal{Z}}(x,t)}{\partial |x|^\gamma}, \Upsilon \rangle - \langle \frac{\partial^\gamma |\mathcal{V}_{\mathcal{Z}}(x,t)|^2}{\partial |x|^\gamma}, \Upsilon \rangle + \langle \Psi(x,t), \Upsilon \rangle = 0. \end{cases} \tag{2.3}$$

To clarify, we define $\tilde{\mathcal{V}}_k^{-1}(t) := \mathcal{F}^{-1}(\tilde{\mathcal{V}}_k(t))$. Applying the FT, we can get:

$$\begin{cases} (\tilde{\mathcal{V}}_{tt})_k(t) - (k)^\gamma \tilde{\mathcal{V}}_k(t) + \tilde{\mathcal{V}}_k(t) + \mathcal{F}\big(\tilde{\mathcal{V}}_k^{-1}(t).\tilde{\mathcal{W}}_k^{-1}(t)\big) + \mathcal{F}\big(|\tilde{\mathcal{V}}_k^{-1}(t)|^2.\tilde{\mathcal{V}}_k^{-1}(t)\big) + \tilde{\Phi}_k(t) = 0, \\ (\tilde{\mathcal{W}}_{tt})_k(t) - (k)^\gamma \tilde{\mathcal{W}}_k(t) - \mathcal{F}\big(|\tilde{\mathcal{V}}_k^{-1}(t)|^2\big) - \tilde{\Psi}_k(t) = 0, \end{cases} \tag{2.4}$$

where $k = -\frac{\mathcal{Z}}{2}, ..., \frac{\mathcal{Z}}{2}$, $0 \leq t \leq t_f$, and $1 < \gamma \leq 2$. The initial conditions are given as:

$$\tilde{\mathcal{V}}_k(0) = (\tilde{\mathcal{V}}_0)_k, \quad (\tilde{\mathcal{V}}_t)_k(0) = (\tilde{z}_0)_k. \quad \tilde{\mathcal{W}}_k(0) = (\tilde{\mathcal{W}}_0)_k, \quad (\tilde{\mathcal{W}}_t)_k(0) = (\tilde{w}_0)_k.$$

Let $\tilde{\mathcal{V}}_t = \tilde{z}$ and $\tilde{\mathcal{W}}_t = \tilde{w}$. Consequently, the fractional KGZ system (2.4) can be expressed in the subsequent manner:

$$\begin{cases} (\tilde{z}_k)_t(t) = \mathcal{N}_z(\tilde{z}_k(t), t), \\ (\tilde{\mathcal{V}}_k)_t(t) = \mathcal{N}_{\mathcal{V}}(\tilde{\mathcal{V}}_k(t), t), \\ (\tilde{w}_k)_t(t) = \mathcal{N}_w(\tilde{w}_k(t), t), \\ (\tilde{\mathcal{W}}_k)_t(t) = \mathcal{N}_{\mathcal{W}}(\tilde{v}_k(t), t), \end{cases} \tag{2.5}$$

where

$$\begin{cases} \mathcal{N}_z(\tilde{z}_k(t), t) = -(k)^\gamma \tilde{\mathcal{V}}_k(t) + \tilde{\mathcal{V}}_k(t) + \mathcal{F}\big(\tilde{\mathcal{V}}_k^{-1}(t).\tilde{\mathcal{W}}_k^{-1}(t)\big) + \mathcal{F}\big(|\tilde{\mathcal{V}}_k^{-1}(t)|^2.\tilde{\mathcal{V}}_k^{-1}(t)\big) + \tilde{\Phi}_k(t), \\ \mathcal{N}_{\mathcal{V}}(\tilde{\mathcal{V}}_k(t), t) = \tilde{z}_k(t), \\ \mathcal{N}_w(\tilde{w}_k(t), t) = -(k)^\gamma \Big(\tilde{\mathcal{W}}_k(t) - \mathcal{F}\big(|\tilde{\mathcal{V}}_k^{-1}(t)|^2\big)\Big) - \tilde{\Psi}_k(t), \\ \mathcal{N}_{\mathcal{W}}(\tilde{v}_k(t), t) = \tilde{w}_k(t). \end{cases}$$

The Equation (2.5) can be addressed using the ETDRK4 method. In the context of the ETDRK4 approach, we examine the equation:

$$\mathcal{V}_t = \mathfrak{L}u + \mathfrak{N}(\mathcal{V}). \tag{2.6}$$

By multiplying Equation (2.6) by $e^{-\mathfrak{L}t}$ and subsequently integrating on $[\tau_n, \tau_{n+1}]$, we find that (2.6) is equivalent to

$$\tilde{\mathcal{V}}_k(\tau_n + \delta t) = e^{\mathfrak{L}\delta t}\tilde{\mathcal{V}}_k(\tau_n) + e^{\mathfrak{L}\delta t}\int_0^{\delta t} e^{-\mathfrak{L}s} \times \mathfrak{N}(\tilde{\mathcal{V}}_k(\tau_n + s), \tau_n + s)ds, \tag{2.7}$$

in which δt represents step size in time direction. To approximate the integral component of (2.7), the fourth-order Runge-Kutta (RK4) technique is employed, leading to the formulation of ETDRK4 as follows [2]:

$$\begin{cases} \eta_n = e^{\frac{\mathfrak{L}\delta t}{2}}\tilde{\mathcal{V}}_{k,n} + \mathfrak{L}^{-1}(e^{\frac{\mathfrak{L}\delta t}{2}} - 1)\mathfrak{N}(\tilde{\mathcal{V}}_{k,n}, \tau_n), \\ \mathcal{V}_n = e^{\frac{\mathfrak{L}\delta t}{2}}\tilde{\mathcal{V}}_{k,n} + \mathfrak{L}^{-1}(e^{\frac{\mathfrak{L}\delta t}{2}} - 1)\mathfrak{N}(\eta_n, \tau_n + \frac{\delta t}{2}), \\ \zeta_n = e^{\frac{\mathfrak{L}\delta t}{2}}\eta_k + \mathfrak{L}^{-1}(e^{\frac{\mathfrak{L}\delta t}{2}} - 1)(2\mathfrak{N}(\mu_n, \tau_n + \frac{\delta t}{2}) - \mathcal{N}(\tilde{\mathcal{V}}_{k,n}, \tau_n)), \\ \tilde{\mathcal{V}}_{k,n+1} = e^{\mathfrak{L}\delta t}\tilde{\mathcal{V}}_{k,n} + \delta t(\rho_1\mathfrak{N}(\tilde{\mathcal{V}}_{k,n}, \tau_n) + 2\rho_2(\mathfrak{N}(\eta_n, \tau_n + \frac{\delta t}{2}) + \mathfrak{N}(\mu_n, \tau_n + \frac{\delta t}{2})) + \rho_3\mathfrak{N}(\zeta_n(\tau_n), \tau_n + \delta t)), \end{cases} \tag{2.8}$$

where

$$\begin{cases} \rho_1 = 4\vartheta_3(\mathfrak{L}\delta t) - 3\vartheta_2(\mathfrak{L}\delta t) + \vartheta_1(L\delta t), \\ \rho_2 = \vartheta_2(\mathfrak{L}\delta t) - 2\vartheta_3(\mathfrak{L}\delta t), \\ \rho_3 = 4\vartheta_3(\mathfrak{L}\delta t) - \vartheta_2(\mathfrak{L}\delta t), \end{cases} \tag{2.9}$$

and the functions $\vartheta_1, \vartheta_2, \vartheta_3$ can be derived from

$$\vartheta_1(z) = \frac{e^z - 1}{z}, \quad \vartheta_2(z) = \frac{e^z - 1 - z}{z^2}, \quad \vartheta_3(z) = \frac{e^z - 1 - z - \frac{z^2}{2}}{z^3}.$$

When $\mathfrak{L}$ approaches zero, the ETDRK4 method experiences numerical instability in this configuration. This issue has been addressed by calculating a contour integral situated away from the origin, as described in [5]. Additionally, an enhanced ETDRK method proposed in [6] demonstrates certain computational advantages over the traditional ETDRK method.

To analyze the stability of the ETDRK4 method, we assume the existence of a fixed point $\mathcal{V}_0$ for the differential Equation (2.6), such that $\mathfrak{L}\mathcal{V}_0 + \mathfrak{N}(\mathcal{V}_0) = 0$. By linearizing around this determined point, if $\mathcal{V}$ denotes the perturbation of $\mathcal{V}_0$ and $\lambda = \mathfrak{N}'(\mathcal{V}_0)$, we obtain

$$\mathcal{V}_t = \mathfrak{L}\mathcal{V} + \lambda\mathcal{V}. \tag{2.10}$$

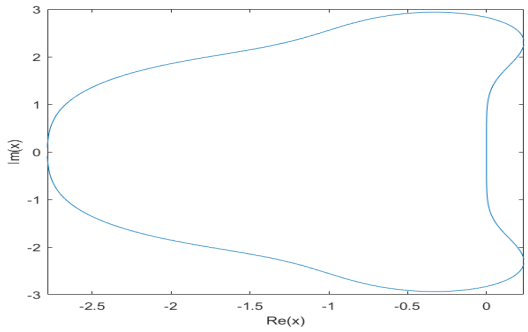

FIGURE 1. The Stability regions for s=0.

When the real part of $C + \lambda$ is negative, the fixed point $\mathcal{V}_0$ demonstrates stability. Applying the ETDRK4 method produces a recurrence relation between $\mathcal{V}n$ and $\mathcal{V}n + 1$. By setting $x = \lambda\delta t$ and $y = \mathfrak{L}\delta t$, the amplification factor is derived as:

$$\frac{\mathcal{V}_{n+1}}{\mathcal{V}_n} = \mathcal{R}(x, s) = d_0 + d_1 x + d_2 x^2 + d_3 x^3 + d_4 x^4,$$

where $d_i, i = 0, \ldots, 4$ are calculated in [3]. For instance, let $d_0 = \mathrm{e}^s$. When s is small, the asymptotic expansions for d_1, d_2, d_3 and d_4 are as follows:

$$\begin{aligned}
d_1 &= 1 + s + \frac{1}{2}s^2 + \frac{1}{2}s^2 + \frac{1}{6}s^3 + \frac{13}{320}s^4 + \frac{17}{960}s^5 + \mathcal{O}(s^6),\\
d_2 &= \frac{1}{2} + \frac{1}{2}s + \frac{1}{4}s^2 + \frac{247}{2880}s^3 + \frac{131}{5760}s^4 + \frac{479}{96768}s^5 + \mathcal{O}(s^6),\\
d_3 &= \frac{1}{6} + \frac{1}{6}s + \frac{61}{720}s^2 + \frac{1}{36}s^3 + \frac{1441}{241920}s^4 + \frac{67}{120960}s^5 + \mathcal{O}(s^6),\\
d_4 &= \frac{1}{24} + \frac{1}{32}s + \frac{7}{640}s^2 + \frac{19}{11520}s^3 - \frac{25}{64512}s^4 - \frac{311}{860160}s^5 + \mathcal{O}(s^6).
\end{aligned}$$

As $s \to 0$, we obtain:

$$\mathcal{R}(x) = 1 + x + \frac{1}{2}x^2 + \frac{1}{6}x^3 + \frac{1}{24}x^4,$$

which represents the amplification ratio for the RK4 method. When $s = 0$, the stability region is presented in the complex plane x in Figure 1.

The following approximation can be derived by employing two differentiation formulas for $j = 0, 1, \ldots, \mathcal{Z} - 1$ [1]:

$$\begin{cases}
\hat{\mathcal{V}}(x_j, \tau_{n+1}) = \delta t z(x_j, \tau_n) + \mathcal{V}(x_j, \tau_n), & n \geq 0,\\
\hat{\mathcal{W}}(x_j, \tau_{n+1}) = \delta t w(x_j, \tau_n) + \mathcal{W}(x_j, \tau_n), & n \geq 0.
\end{cases} \tag{2.11}$$

To implement the ETDRK4 method for the system described in (2.5), it is necessary to obtain the values of functions at the midpoint of the intervals. Consequently, we can use the subsequent linear interpolation method:

$$\begin{cases}
\bar{\mathcal{V}}(x_j, t) = \mathcal{V}(x_j, \tau_n) + \frac{\mathcal{V}(x_j, \tau_{n+1}) - \mathcal{V}(x_j, \tau_n)}{\tau_{n+1} - \tau_n}(t - \tau_n),\\
\bar{\mathcal{W}}(x_j, t) = \mathcal{W}(x_j, \tau_n) + \frac{\mathcal{W}(x_j, \tau_{n+1}) - \mathcal{W}(x_j, \tau_n)}{\tau_{n+1} - \tau_n}(t - \tau_n).
\end{cases} \tag{2.12}$$

For simplification, let us define $\tilde{\mathcal{V}}_{n,k}^{-1} := \mathcal{F}^{-1}(\tilde{\mathcal{V}}_k(\tau_n))$. By applying the ETDRK4 method along with Equations (2.11) and (2.12), we can derive:

$$\begin{cases}\mathcal{N}_z(\tau_n) = -(k)^\gamma\tilde{\mathcal{V}}_{n,k} + \tilde{\mathcal{V}}_{n,k} + \mathcal{F}\big(\tilde{\mathcal{V}}_{n,k}^{-1}.\tilde{\mathcal{W}}_{n,k}^{-1}\big) + \mathcal{F}\big(|\tilde{\mathcal{V}}_{n,k}^{-1}|^2.\tilde{\mathcal{V}}_{n,k}^{-1}\big) + \tilde{\Phi}_{n,k},\\ \mathcal{N}_z(\tau_{n+\frac{1}{2}}) = -(k)^\gamma(\tilde{\mathcal{V}}_{n,k} + \frac{\delta t}{2}\tilde{z}_{n,k}) + \tilde{\mathcal{V}}_{n,k} + \frac{\delta t}{2}\tilde{z}_{n,k} + \mathcal{F}\big((\tilde{\mathcal{V}}_{n,k}^{-1} + \frac{\delta t}{2}\tilde{z}_{n,k}).(\tilde{\mathcal{W}}_{n,k}^{-1} + \frac{\delta t}{2}\tilde{w}_{n,k})\big)\\ \qquad +\mathcal{F}\big(|\tilde{\mathcal{V}}_{n,k}^{-1} + \frac{\delta t}{2}\tilde{z}_{n,k}|^2.(\tilde{\mathcal{V}}_{n,k}^{-1} + \frac{\delta t}{2}\tilde{z}_{n,k})\big) + \tilde{\Phi}_{n+\frac{1}{2},k} = 0,\\ \mathcal{N}_z(\tau_{n+1}) = -(k)^\gamma(\tilde{\mathcal{V}}_{n,k} + \delta t\tilde{z}_{n,k}) + \tilde{\mathcal{V}}_{n,k} + \delta t\tilde{z}_{n,k} + \mathcal{F}\big((\tilde{\mathcal{V}}_{n,k}^{-1} + \delta t\tilde{z}_{n,k}).(\tilde{\mathcal{W}}_{n,k}^{-1} + \delta t\tilde{w}_{n,k})\big)\\ \qquad + \mathcal{F}\big(|\tilde{\mathcal{V}}_{n,k}^{-1} + \delta t\tilde{z}_{n,k}|^2.(\tilde{\mathcal{V}}_{n,k}^{-1} + \delta t\tilde{z}_{n,k})\big) + \tilde{\Phi}_{n+1,k} = 0,\\ \tilde{z}_{n+1,k} = \tilde{z}_{n,k} + \Omega_1\mathcal{N}_z(\tau_n) + 4\Omega_2\mathcal{N}_z(\tau_{n+\frac{1}{2}}) + \Omega_3\mathcal{N}_z(\tau_{n+1}).\end{cases}$$

In this context, $\tilde{z}_{n,k} = \tilde{z}_k(\tau_n)$ and

$$\begin{cases}\Omega_1 = \delta t^{-2}\mathfrak{L}^{-3}\Big(-4 - \mathfrak{L}\delta t + e^{\mathfrak{L}\delta t}(4 - 3\mathfrak{L}\delta t + (\mathfrak{L}\delta t)^2)\Big),\\ \Omega_2 = \delta t^{-2}\mathfrak{L}^{-3}\Big(2 + \mathfrak{L}\delta t + e^{\mathfrak{L}\delta t}(-2 + (\mathfrak{L}\delta t))\Big),\\ \Omega_3 = \delta t^{-2}\mathfrak{L}^{-3}\Big(-4 - 3\mathfrak{L}\delta t + e^{\mathfrak{L}\delta t}(4 - \mathfrak{L}\delta t - (\mathfrak{L}\delta t)^2)\Big).\end{cases}$$

However, since $\mathfrak{L} = 0$, we will implement the method proposed in [5]. By performing the inverse FT, we can approximate the solution for $z(x_j, \tau_{n+1})$. Given that $\mathcal{N}_u = \tilde{z}_{n,k}$, we can express:

$$\tilde{\mathcal{V}}_{n+1,k} \quad = \quad \tilde{\mathcal{V}}_{n,k} + \Omega_1\tilde{z}_{n,k} + 2\Omega_2\tilde{z}_{n,k} + (2\Omega_2 + \Omega_3)\tilde{z}_{n+1,k}. \tag{2.13}$$

Moreover, since $\mathcal{N}_w$ is not dependent on $\tilde{w}_{n,k}$, we can determine $\tilde{w}_{n+1,k}$ as below:

$$\begin{cases}\mathcal{N}_w(\tau_n) = -(k)^\gamma\tilde{\mathcal{W}}_{n,k} - \mathcal{F}\big(|\tilde{\mathcal{V}}_{n,k}^{-1}(t)|^2\big) - \tilde{\Psi}_{n,k},\\ \mathcal{N}_w(\tau_{n+\frac{1}{2}}) = -(k)^\gamma(\tilde{\mathcal{W}}_{n,k} + \frac{\delta t}{2}\tilde{w}_{n,k}) - \mathcal{F}\big(|\tilde{\mathcal{V}}_{n,k}^{-1} + \frac{\delta t}{2}\tilde{z}_{n,k}|^2\big) - \tilde{\Psi}_{n+\frac{1}{2},k},\\ \mathcal{N}_w(\tau_{n+1}) = -(k)^\gamma(\tilde{\mathcal{W}}_{n,k} + \delta t\tilde{w}_{n,k}) - \mathcal{F}\big(|\tilde{\mathcal{V}}_{n,k}^{-1} + \delta t\tilde{z}_{n,k}|^2\big) - \tilde{\Psi}_{n+1,k},\\ \tilde{w}_{n+1,k} = \tilde{w}_{n,k} + \Omega_1\mathcal{N}_w(\tau_n) + 4\Omega_2\mathcal{N}_w(\tau_{n+\frac{1}{2}}) + \Omega_3\mathcal{N}_w(\tau_{n+1}).\end{cases}$$

By applying the inverse FT, we can approximate the solution for $w(x_j, \tau_{n+1})$. Given that $\mathcal{N}_v = \tilde{w}_{n,k}$, we can derive:

$$\tilde{\mathcal{W}}_{n+1,k} \quad = \quad \tilde{\mathcal{W}}_{n,k} + \Omega_1\tilde{w}_{n,k} + 2\Omega_2\tilde{w}_{n,k} + (2\Omega_2 + \Omega_3)\tilde{w}_{n+1,k}.$$

Ultimately, by using the inverse FT, we can approximate the solution for $\mathcal{W}(x_j, \tau_{n+1})$. For $n = 0$, the first equation in (2.11) has been used.

Theorem 2.1. *Suppose $\tilde{\mathcal{V}}_k(t), \tilde{\mathcal{W}}_k(t)$ be the obtained solutions of (2.4) using ETDRK4 method and $\hat{\tilde{\mathcal{V}}}_k(t), \hat{\tilde{\mathcal{W}}}_k(t)$ be the approximate solutions of (2.4) given by Equations (2.11) and (2.12). If $\tilde{\mathcal{V}}_k(t_n) - \hat{\tilde{\mathcal{V}}}_k(t_n) = \widetilde{e\mathcal{V}}_{n,k}$ and $\tilde{\mathcal{W}}_k(t_n) - \hat{\tilde{\mathcal{W}}}_k(t_n) = \widetilde{e\mathcal{W}}_{n,k}$, then we have*

$$|\widetilde{e\mathcal{V}}_{n,k}| = \mathcal{O}(\delta t^2), \qquad |\widetilde{e\mathcal{W}}_{n,k}| = \mathcal{O}(\delta t^2).$$

Proof. According to ETDRK4, we have

$$\begin{cases}\tilde{z}_{n+1,k} = \tilde{z}_{n,k} + \Omega_1\mathcal{N}_z(\tau_n) + 4\Omega_2\mathcal{N}_z(\tau_{n+\frac{1}{2}}) + \Omega_3\mathcal{N}_z(\tau_{n+1}).\\ \tilde{\mathcal{V}}_{n+1,k} = \tilde{\mathcal{V}}_{n,k} + \Omega_1\tilde{z}_{n,k} + 2\Omega_2\tilde{z}_{n,k} + (2\Omega_2 + \Omega_3)\tilde{z}_{n+1,k}.\\ \tilde{w}_{n+1,k} = \tilde{w}_{n,k} + \Omega_1\mathcal{N}_w(\tau_n) + 4\Omega_2\mathcal{N}_w(\tau_{n+\frac{1}{2}}) + \Omega_3\mathcal{N}_w(\tau_{n+1}).\\ \tilde{\mathcal{W}}_{n+1,k} = \tilde{\mathcal{W}}_{n,k} + \Omega_1\tilde{w}_{n,k} + 2\Omega_2\tilde{w}_{n,k} + (2\Omega_2 + \Omega_3)\tilde{w}_{n+1,k}.\end{cases}$$

Since $2\Omega_2+\Omega_3=\mathcal{O}(\delta t)$, therefore, we have

$$\begin{cases}\tilde{z}_{n+1,k}=\tilde{z}_{n,k}+(\Omega_1+4\Omega_2+\Omega_3)((1-(k)^{\gamma})\tilde{\mathcal{V}}_{n,k}+\mathcal{F}\big(\tilde{\mathcal{V}}_{n,k}^{-1}.\tilde{\mathcal{W}}_{n,k}^{-1}\big)\\ \qquad\qquad +\mathcal{F}\big(|\tilde{\mathcal{V}}_{n,k}^{-1}|^2.\tilde{\mathcal{V}}_{n,k}^{-1}\big)+\Omega_1\tilde{\Phi}_{n,k}+4\Omega_2\tilde{\Phi}_{n+\frac{1}{2},k}+\Omega_3\tilde{\Phi}_{n+1,k}+\mathcal{O}(\delta t^2),\\ \tilde{\mathcal{V}}_{n+1,k}=\tilde{\mathcal{V}}_{n,k}+\Omega_1\tilde{z}_{n,k}+2\Omega_2\tilde{z}_{n,k}+(2\Omega_2+\Omega_3)\tilde{z}_{n+1,k},\\ \tilde{w}_{n+1,k}=\tilde{w}_{n,k}+(\Omega_1+4\Omega_2+\Omega_3)(-(k)^{\gamma}\tilde{\mathcal{W}}_{n,k}-\mathcal{F}\big(|\tilde{\mathcal{V}}_{n,k}^{-1}(t)|^2\big)\\ \qquad\qquad -\Omega_1\tilde{\Psi}_{n,k}+4\Omega_2\tilde{\Psi}_{n+\frac{1}{2},k}+\Omega_3\tilde{\Psi}_{n+1,k}+\mathcal{O}(\delta t^2),\\ \tilde{\mathcal{W}}_{n+1,k}=\tilde{\mathcal{W}}_{n,k}+\Omega_1\tilde{w}_{n,k}+2\Omega_2\tilde{w}_{n,k}+(2\Omega_2+\Omega_3)\tilde{w}_{n+1,k}.\end{cases}$$

Let n=0, since $\widetilde{e\mathcal{W}}_{0,k}=\widetilde{e\mathcal{V}}_{0,k}=0$ we can conclude that $\widetilde{e\mathcal{W}}_{1,k}$ and $\widetilde{e\mathcal{V}}_{1,k}$ are $\mathcal{O}(\delta t^2)$. The proof is concluded by employing induction. □

Theorem 2.2. *Let $\mathcal{V}(x,t),\mathcal{W}(x,t)$ denote the exact solutions of the system (1.1) while $\mathcal{V}_N(x,t),\mathcal{W}_N(x,t)$ represent the approximate solutions derived from the proposed method. If $\mathcal{V}(x_j,t_n)-\mathcal{V}_N(x_j,t_n)=e_{n,j}$ and $\mathcal{W}(x_j,t_n)-\mathcal{W}_N(x_j,t_n)=E_{n,j}$, then we have*

$$|e_{n,j}|=\mathcal{O}(\delta t^2),\qquad |E_{n,j}|=\mathcal{O}(\delta t^2).$$

Proof. Define $\mathcal{V}_N^{RK}(x_j,t_n)=\sum_{k=-\frac{N}{2}}^{\frac{N}{2}}\tilde{\mathcal{V}}_k(t_n)\mathrm{e}^{ikx_j}$, $\mathcal{V}_N(x_j,t_n)=\sum_{k=-\frac{N}{2}}^{\frac{N}{2}}\hat{\tilde{\mathcal{V}}}_k(t_n)\mathrm{e}^{ikx_j}$, and consider Theorem 2.1, then we have

$$\mathcal{V}_N^{RK}(x_j,t_n)-\mathcal{V}_N(x_j,t_n)=\sum_{k=-\frac{N}{2}}^{\frac{N}{2}}\tilde{e}_{n,k}\mathrm{e}^{ikx_j}=\mathcal{O}(\delta t^2).$$

By applying triangle inequality we have

$$|\mathcal{V}(x_j,t_n)-\mathcal{V}_N(x_j,t_n)|\le|\mathcal{V}(x_j,t_n)-\mathcal{V}_N^{RK}(x_j,t_n)|+|\mathcal{V}_N^{RK}(x_j,t_n)-\mathcal{V}_N(x_j,t_n)|.$$

Given that the ETDRK4 method is of fourth order, the desired results can be attained. □

3. Numerical examples

This section presents several numerical simulations and comparisons to check the efficiency and accuracy of the studied method. The root mean square errors (RMSE) and maximum absolute errors (MAE) are presented to measure the accuracy of the proposed method. The examples are solved using various time step values and different fractional orders. The tables also include the algorithm's execution time and convergence ratio for different values of time steps.

Example 3.1. *Consider a one-dimensional KGZ system as the first example as follwos[11]:*

$$\begin{cases}\mathcal{V}_{tt}(\boldsymbol{x},t)-\frac{\partial^{\gamma}\mathcal{V}}{\partial|x|^{\gamma}}(\boldsymbol{x},t)+\mathcal{V}(\boldsymbol{x},t)+\mathcal{W}(\boldsymbol{x},t)\mathcal{V}(\boldsymbol{x},t)+|\mathcal{V}(\boldsymbol{x},t)|^2\mathcal{V}(\boldsymbol{x},t)=0, & (\boldsymbol{x},t)\in\mathbb{R}\times(0,t_f],\\ \mathcal{W}_{tt}(\boldsymbol{x},t)-\frac{\partial^{\gamma}\mathcal{W}}{\partial|x|^{\gamma}}(\boldsymbol{x},t)-\frac{\partial^{\gamma}(|\mathcal{V}|^2)}{\partial|x|^{\gamma}}(\boldsymbol{x},t)=0, & (\boldsymbol{x},t)\in\mathbb{R}\times(0,t_f],\\ (\mathcal{V},\phi)(\boldsymbol{x},t)=0, & (\boldsymbol{x},t)\in\{-\infty,\infty\}\times(0,t_f],\\ (\mathcal{V},\mathcal{V}_t,\mathcal{V},\mathcal{W}_t)(\boldsymbol{x},t)=(\mathcal{V}_0,\mathcal{V}_1,\mathcal{W}_0,\mathcal{W}_1)(\boldsymbol{x}), & (\boldsymbol{x},t)\in\mathbb{R}\times\{t=0\}.\end{cases}\tag{3.1}$$

Let $\gamma=2$ and

$$\begin{cases}\mathcal{V}_0=\frac{\sqrt{10}-\sqrt{2}}{2}sech\Big(\sqrt{\frac{1+\sqrt{5}}{2}}x\Big).\exp\Big[i\Big(\sqrt{\frac{2}{1+\sqrt{5}}}x\Big)\Big],\\ \mathcal{V}_t=\frac{\sqrt{10}-\sqrt{2}}{2}sech\Big(\sqrt{\frac{1+\sqrt{5}}{2}}x\Big)tanh(\sqrt{\frac{1+\sqrt{5}}{2}}x)-\frac{\sqrt{10}-\sqrt{2}}{2}sech\Big(\sqrt{\frac{1+\sqrt{5}}{2}}x\Big).\exp\Big[i\Big(\sqrt{\frac{2}{1+\sqrt{5}}}x\Big)\Big],\\ \mathcal{W}_0=-2sech^2\Big(\sqrt{\frac{1+\sqrt{5}}{2}}x\Big),\\ \mathcal{W}_t=-4sech^2\Big(\sqrt{\frac{1+\sqrt{5}}{2}}x\Big)tanh(\sqrt{\frac{1+\sqrt{5}}{2}}x\Big).\end{cases}\tag{3.2}$$

TABLE 1. The $RMSE$ and convergence rate with $\mathcal{Z} = 128$ and $\gamma = 2$ at $t_f = 1$ (Example 3.1).

	$\mathcal{V}(x,t)$		$\mathcal{W}(x,t)$	
δt	$RMSE$	$Ratio$	$RMSE$	$Ratio$
0.10000	$8.2971e{-4}$	–	$5.7760e{-4}$	–
0.05000	$2.4561e{-4}$	1.7562	$1.5636e{-4}$	1.8851
0.02500	$6.7219e{-5}$	1.8694	$4.1775e{-5}$	1.9042
0.01250	$1.7753e{-5}$	1.9208	$1.0496e{-5}$	1.9927
0.00625	$4.5627e{-6}$	1.96014	$2.6247e{-6}$	1.9997

TABLE 2. The $RMSEs$ and convergence rate with $\delta t = 0.001$ and $\gamma = 2$ at $t_f = 1$ (Example 3.1).

	$\mathcal{V}(x,t)$		$\mathcal{W}(x,t)$	
$\mathcal{Z}$	$RMSE$	$Ratio$	$RMSE$	$Ratio$
8	$7.2894e{-1}$	–	$6.2384e{-1}$	–
16	$4.7410e{-1}$	0.6208	$3.7546e{-1}$	0.7325
32	$1.9999e{-1}$	1.2452	$1.5716e{-1}$	1.3194
64	$1.0034e{-3}$	4.3169	$7.5160e{-3}$	4.3862
128	$1.0059e{-7}$	13.2841	$2.5411e{-7}$	14.8522

The exact solution to the above problem is as follows:

$$\begin{cases} \mathcal{V}(\boldsymbol{x},t) = \frac{\sqrt{10}-\sqrt{2}}{2} sech\Big(\sqrt{\frac{1+\sqrt{5}}{2}}x - t\Big).\exp\Big[i\Big(\sqrt{\frac{2}{1+\sqrt{5}}}x - t\Big)\Big], \\ \mathcal{W}(\boldsymbol{x},t) = -2sech^2\Big(\sqrt{\frac{1+\sqrt{5}}{2}}x - t\Big). \end{cases} \tag{3.3}$$

We solve Equation (3.1) with $-10 \leq x \leq 10$. Second-order accuracy compared to the time step and spectral accuracy compared to the spatial step can be seen according to the results reported in Tables 1 and 2.

In the absence of the exact solution when $1 < \gamma < 2$ for Example 3.1, we define the error as follows:

$$error := \max_{0\leq m\leq \mathcal{Z}} \max_{0\leq n\leq s} |\mathcal{V}_{n,m} - \hat{\mathcal{V}}_{n,\hat{m}}|,$$

where $\hat{\mathcal{V}}$ is obtained using a refined temporal using $\delta t/2$ as step size in time direction and $\hat{m} = 2m$. Tables 3 and 4 report the convergence rates, RMSE, MAE, and CPU times for various values of γ and δt with $\mathcal{Z} = 128$ at $t_f = 10$. The results show that the convergence rate is close to two.

The numerical solutions of $|\mathcal{V}(x,t)|$, $\text{Real}(\mathcal{V}(x,t))$, $\text{Im}(\mathcal{V}(x,t))$, and $\mathcal{W}(x,t)$ are illustrated in Figure 2 with $\delta t = 0.001$ and $\mathcal{Z} = 128$ for Example 3.1 when $\gamma = 2$. In Figure 3 the MAE of the approximations of $\mathcal{V}(x,t)$ and $\mathcal{W}(x,t)$ using $\delta t = 0.0001$ and $\mathcal{Z} = 128$ for $\gamma = 2$ at $t_f = 10$ are illustrated. The reported results for this example show the efficiency and accuracy of the proposed method.

Example 3.2. *The following system of nonlinear KGZ equations, which contains the space-fractional operators, is considered in this example:*

$$\begin{cases} \frac{\partial^2 \mathcal{V}}{\partial t^2} - \frac{\partial^\gamma \mathcal{V}}{\partial |x|^\gamma} + \mathcal{V} + \mathcal{W}\mathcal{V} + |\mathcal{V}|^2\mathcal{W} = 0, & (x,t) \in \mathbb{R} \times (0,t_f], t_f > 0, \\ \frac{\partial^2 \mathcal{W}}{\partial t^2} - \frac{\partial^\gamma \mathcal{W}}{\partial |x|^\gamma} - \frac{\partial^\gamma (|\mathcal{V}|^2)}{\partial |x|^\gamma} = 0, & (x,t) \in \mathbb{R} \times (0,t_f], t_f > 0, \end{cases}$$

in which $x \in [0,1], t \in [0,1]$ *and* $1 < \gamma \leq 2$. *Let the initial conditions be as follows:*

$$\mathcal{V}(x,0) = sin2\pi x, \quad \mathcal{V}_t(x,0) = sin2\pi x, \quad \mathcal{W}(x,0) = 0, \quad \mathcal{W}_t(x,0) = cos2\pi x, \ 0 \leq x \leq 1.$$

TABLE 3. The MAE, $RMSE$, convergence rate, and CPU time for $\mathcal{V}(x,t)$ with $\mathcal{Z}=128$ and various δt at $t_f=10$ (Example 3.1).

γ	δt	MAE	$Ratio$	$RMSE$	$CPU(s)$
1.1	0.0100	$7.40085856e{-5}$	–	$2.26274564e{-6}$	16.0292
	0.0050	$1.74139881e{-5}$	2.0874	$8.21207837e{-7}$	63.0353
	0.0025	$4.27651124e{-6}$	2.0257	$2.39504362e{-7}$	218.0736
1.2	0.0100	$7.36041148e{-5}$	–	$2.26218284e{-6}$	16.0211
	0.0050	$1.72249137e{-5}$	2.1011	$8.11758336e{-7}$	57.0.0361
	0.0025	$4.22291887e{-6}$	2.0282	$2.34450326e{-7}$	179.0.0712
1.4	0.0100	$7.36038528e{-5}$	–	$2.26023864e{-6}$	15.0182
	0.0050	$1.67409487e{-5}$	2.1364	$7.87501943e{-7}$	53.0393
	0.0025	$4.08597762e{-6}$	2.0346	$2.21599438e{-7}$	167.0688

TABLE 4. The MAE, $RMSE$, convergence rate, and CPU time for $\mathcal{W}(x,t)$ with $\mathcal{Z}=128$ and various δt at $t_f=10$ (Example 3.1).

γ	δt	MAE	$Ratio$	$RMSE$	$CPU(s)$
1.3	0.0100	$8.23508246e{-5}$	–	$3.82163209e{-6}$	17.9435
	0.0050	$2.06574161e{-5}$	1.9951	$9.55532297e{-6}$	65.3441
	0.0025	$5.16989692e{-6}$	1.9984	$2.38885969e{-6}$	220.5129
1.5	0.0100	$8.17614598e{-5}$	–	$3.92563726e{-6}$	17.8803
	0.0050	$2.04772663e{-5}$	1.9973	$9.81341291e{-7}$	58.3542
	0.0025	$5.11994448{-6}$	1.9998	$2.44444164e{-7}$	181.8493
1.8	0.0100	$8.06021163e{-5}$	–	$3.29586129e{-6}$	5.2969
	0.0050	$2.01376636e{-5}$	2.0009	$8.21399245e{-7}$	19.1197
	0.0025	$4.99682644e{-6}$	2.0108	$2.03787225e{-7}$	67.1354

This example has the following exact solutions

$$\mathcal{V}(x,t)=\mathrm{e}^{t}sin2\pi x, \mathcal{W}(x,t)=(t^2+t)cos2\pi x.$$

In Tables 5 and 6, the MAE, $RMSE$, convergence rates, and CPU time for the approximate solutions of $\mathcal{V}(x,t)$ and $\mathcal{W}(x,t)$ with $\mathcal{Z}=32$ and various values of γ and δt at $t_f=1$ are reported. These results clearly indicate that the convergence rates are nearly two. The absolute errors of the approximate solutions of $\mathcal{V}(x,t)$ and $\mathcal{W}(x,t)$ for Example 3.2 with $\delta t=0.001$, $\mathcal{Z}=64$ and various values of γ at $t_f=1$ are illustrated in Figures 4.

4. Conclusion

This paper presented an efficient and accurate numerical method for solving the nonlinear space-fractional Klein-Gordon-Zakharov system, effectively incorporating the fractional Laplacian operator. This method contributed significantly to the field by preserving mass and energy, which are essential requirements for analyzing such complex systems. By employing the Fourier spectral method for spatial discretization of the problem, the approach leverages the advantages of spectral techniques, which are known for their high accuracy and rapid convergence. Additionally, the incorporation of the ETDRK4 technique for temporal discretization enhances the overall stability and efficiency of the

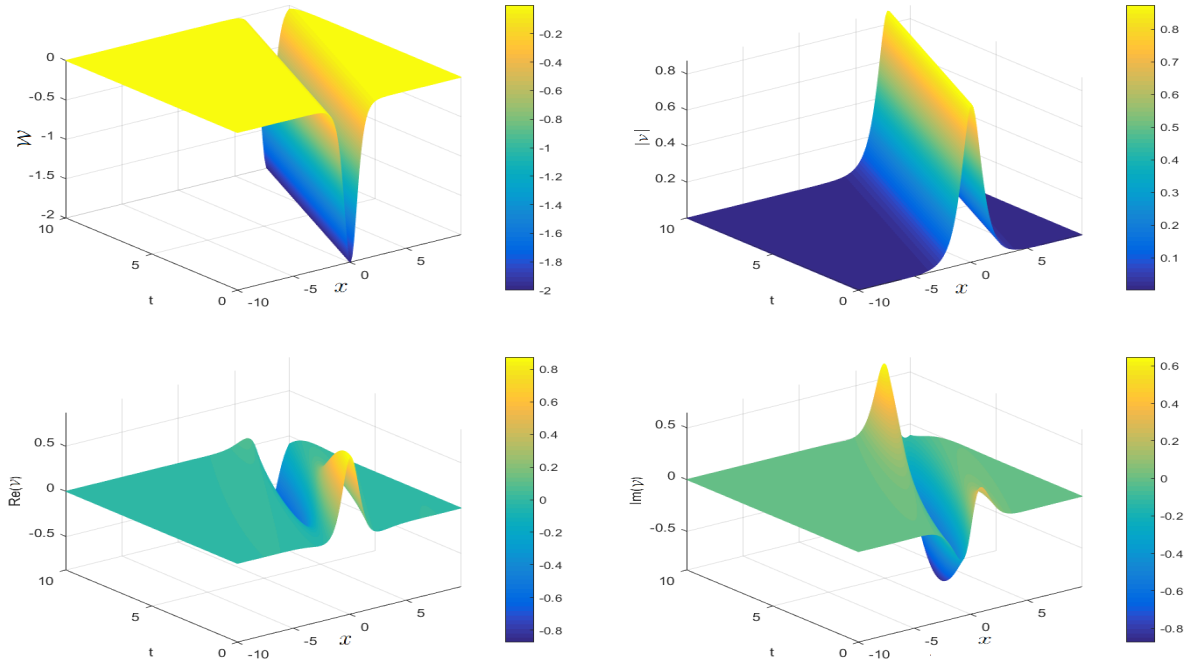

FIGURE 2. The graph of the numerical solutions of $|\mathcal{V}(x,t)|$, Real$(\mathcal{V}(x,t))$, Im$(\mathcal{V}(x,t))$, and $\mathcal{W}(x,t)$ with $\gamma = 2$, $\delta t = 0.001$, and $\mathcal{Z} = 128$ for Example 3.1.

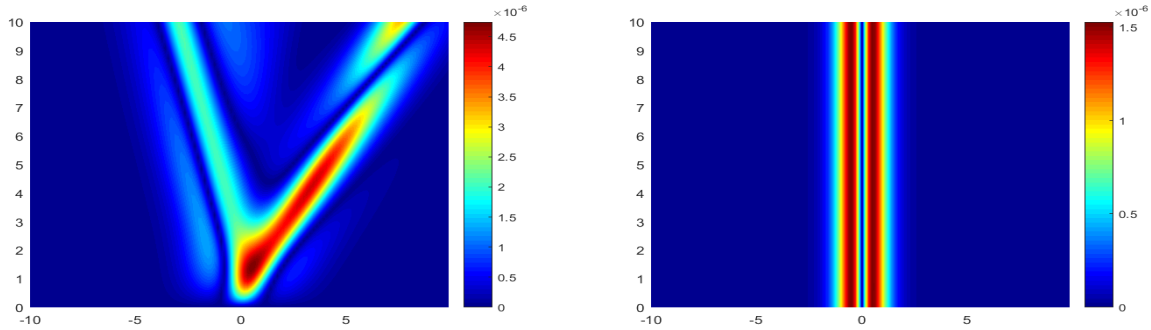

FIGURE 3. Errors of $\mathcal{V}(x,t)$ (left) and $\mathcal{W}(x,t)$ (right) with $\delta t = 0.001$, $\mathcal{Z} = 128$ for $\gamma = 2$ at $t_f = 10$ (Example 3.1).

numerical solution. The convergence proof and detailed numerical experiments demonstrated the method's accuracy and reliability in addressing related problems. The results obtained provided a solid foundation for future research in solving nonlinear space-fractional systems and enhanced the understanding of the behavior of these systems.

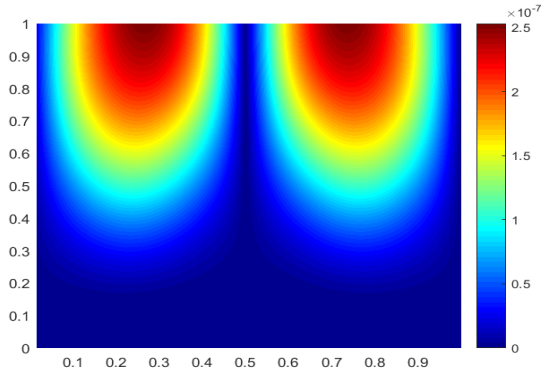

(a) $\gamma = 1.3$.

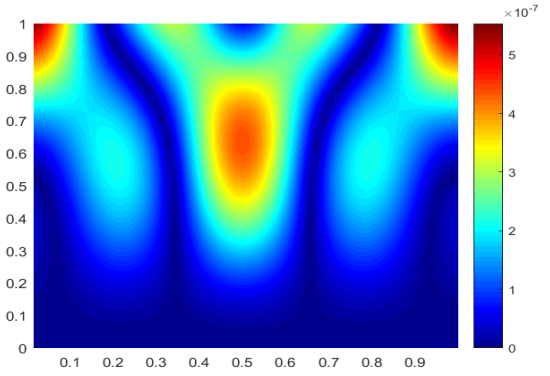

(b) $\gamma = 1.3$.

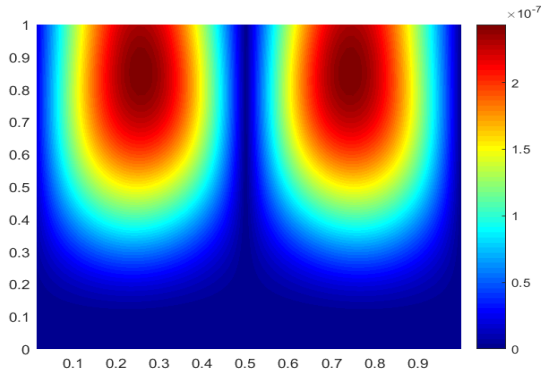

(c) $\gamma = 1.6$.

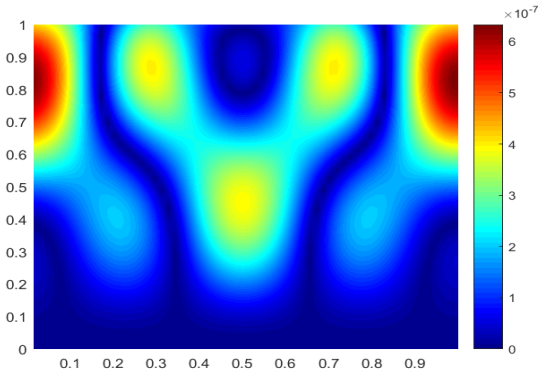

(d) $\gamma = 1.6$.

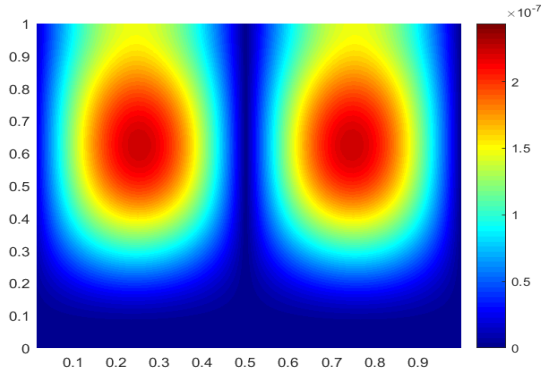

(e) $\gamma = 1.9$

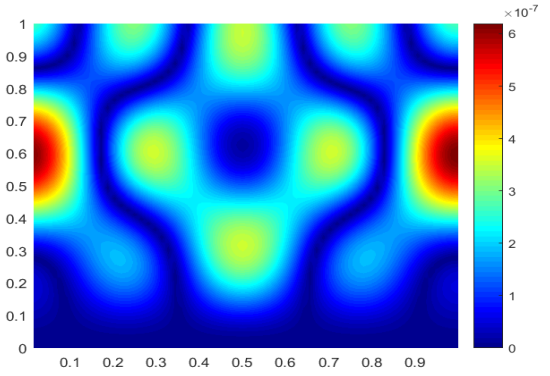

(f) $\gamma = 1.9$.

FIGURE 4. Errors of $\mathcal{V}(x,t)$ (left) and $\mathcal{W}(x,t)$ (right) with $\delta t = 0.001$, $\mathcal{Z} = 64$, and various values of γ at $t_f = 1$ (Example 3.2).

TABLE 5. The MAE, $RMSE$, convergence rate, and CPU time for $\mathcal{V}(x,t)$ with $\mathcal{Z}=32$ at $t_f=1$ (Example 3.2).

γ	δt	MAE	$Ratio$	$RMSE$	$CPU(s)$
1.1	0.0050	$5.99352482e{-6}$	–	$4.49339246e{-6}$	0.2645
	0.0025	$1.50824461e{-6}$	1.9905	$1.13185572e{-6}$	0.4074
	0.0013	$3.78292923e{-7}$	1.9953	$2.84014636e{-7}$	0.8001
	0.0006	$9.47271434e{-8}$	1.9977	$7.11342126e{-8}$	1.8750
1.5	0.0050	$6.25846369e{-6}$	–	$4.32817331e{-6}$	0.2548
	0.0025	$1.56503079e{-6}$	1.9996	$1.08054487e{-6}$	0.3875
	0.0013	$3.91310257e{-7}$	1.9998	$2.69946981e{-7}$	0.7875
	0.0006	$9.78342518e{-8}$	1.9999	$6.74630185e{-8}$	1.8804
1.7	0.0050	$5.93529585e{-6}$	–	$3.60428265e{-6}$	0.2044
	0.0025	$1.48166903e{-6}$	2.0021	$8.95765713e{-7}$	0.3749
	0.0013	$3.70169144e{-7}$	2.0010	$2.23307687e{-7}$	0.7770
	0.0006	$9.25128276e{-7}$	2.0005	$5.57495892e{-8}$	1.8663

TABLE 6. The MAE, $RMSE$, convergence rate, and CPU time for $\mathcal{W}(x,t)$ with $\mathcal{Z}=32$ at $t_f=1$ (Example 3.2).

γ	δt	MAE	$Ratio$	$RMSE$	$CPU(s)$
1.2	0.0050	$1.15688677e{-5}$	–	$5.75519899e{-6}$	0.2942
	0.0025	$2.86516161e{-6}$	2.0136	$1.45246744e{-6}$	0.3951
	0.0013	$7.12952959e{-7}$	2.0067	$3.64943180e{-7}$	0.7994
	0.0006	$1.77823683e{-7}$	2.0034	$9.1471128e{-8}$	1.8804
1.4	0.0050	$1.55280043e{-5}$	–	$7.91802332e{-6}$	0.2325
	0.0025	$3.87984413e{-6}$	2.0008	$1.98940529e{-7}$	0.4008
	0.0013	$9.69607719e{-7}$	2.0005	$4.98471719e{-7}$	0.7813
	0.0006	$2.42352675e{-7}$	2.0003	$1.24750618e{-8}$	1.8608
1.8	0.0050	$1.57488073e{-5}$	–	$4.74756546e{-6}$	0.1939
	0.0025	$3.9266560e{-6}$	2.0039	$1.22225566e{-6}$	0.3679
	0.0013	$9.80459556e{-7}$	2.0018	$3.09952643e{-7}$	0.7583
	0.0006	$2.44973106e{-7}$	2.0008	$7.80335720e{-8}$	1.8564

REFERENCES

[1] K. E. Atkinson, *An Introduction to Numerical Analysis*, Willey, Canada, 1978.

[2] S. M. Cox and P. C. Matthews, *Exponential time differencing for stiff systems*, J. Comput. Phys., *176* (2002), 430–455.

[3] F. De and F. Vadillo, *An exponential time differencing method for the nonlinear Schrödinger equation*, Comput. Phys. Commun., *179*(7) (2008), 449–456.

[4] A. S. Hendy and J. E. Macías-Díaz, *A numerically efficient and conservative model for a Riesz space-fractional Klein-Gordon-Zakharov system*, Commun. Nonlinear Sci. Numer., *71* (2019), 22–37.

[5] A. Kassam and L. N. Trefethen, *Fourth-order time stepping for stiff PDEs*, SIAM J. Sci. Comput., *26* (2005), 1214–1233.
[6] X. Liang, A. Q. M. Khaliq, and Y. Xing, *Fourth Order Exponential Time Differencing Method with Local Discontinuous Galerkin Approximation for Coupled Nonlinear Schrödinger Equations*, Commun. Comput. Phys., *17*(2) (2015), 510–541.
[7] Y. F. Luchko, H. Martínez, and J. J. Trujillo, *Fractional Fourier transform and some of its applications*, Fract. Calc. Appl. Anal., *11*(4) (2008), 457–470.
[8] N. A. Larkin and M. V. Padilha, *Global Regular Solutions to One Problem of Saut-Temam for the 3D Zakharov-Kuznetsov Equation*, APPL. MATH. OPT., *77*(2) (2016), 253–274.
[9] J. E. Macías-Díaz, *Existence of solutions of an explicit energy-conserving scheme for a fractional Klein-Gordon-Zakharov system*, Appl. Numer. Math., *151* (2020), 40–43.
[10] R. Martínez, J.E. Macías-Díaz, and A. S. Hendy, *Theoretical analysis of an explicit energy-conserving scheme for a fractional Klein-Gordon-Zakharov system*, Appl. Numer. Math., *146* (2019), 245–259.
[11] R. Martínez and J. E. Macías-Díaz, *An energy-preserving and efficient scheme for a double-fractional conservative Klein-Gordon-Zakharov system*, Appl. Numer. Math., *158* (2020), 292–313.
[12] S. Mohammadi, M. Fardi, and M. Ghasemi, *A numerical investigation with energy-preservation for nonlinear space-fractional Klein-Gordon-Schrödinger system*, Comput. Appl. Math., *42*(8) (2023), 356.
[13] S. Saha Ray and S. Sahoo, *Comparison of two reliable analytical methods based on the solutions of fractional coupled Klein-Gordon-Zakharov equations in plasma physics*, Comput. Math. Math. Phys., *56*(7) (2016), 1319–1335.
[14] S. Sahoo and S. Saha Ray, *Improved fractional sub-equation method for (3+1)-dimensional generalized fractional KdV-Zakharov-Kuznetsov equations*, Comput. Math. Appl., *70*(2) (2015), 158–166.
[15] J. Shen, T. Tang, and L. Wang, *Spectral methods: Algorithms, analysis and applications*, Springer, Germany, 2011.
[16] C. Sun and L. Li, *The Global Existence and Uniqueness of the Classical Solution with the Periodic Initial Value Problem for One-Dimension Klein-Gordon-Zakharov Equations*, Adv. Math. Phys., *2018*(1) (2018), 4820601.
[17] K. L. Wang, *Novel approaches to fractional Klein–Gordon–Zakharov equation*, Fractals, *31*(07) (2023), 2350095.
[18] C. Xie and S. Fang, *Efficient numerical methods for Riesz space-fractional diffusion equations with fractional Neumann boundary conditions*, Appl. Numer. Math., *176* (2022), 1–18.
[19] J. Xie and Z. Zhang, *An analysis of implicit conservative difference solver for fractional Klein-Gordon-Zakharov system*, Appl. Math. Comput., *348* (2019), 153-166.
[20] S. You and X. Ning, *On global smooth solution for generalized Zakharov equations*, Comput. Math. Appl., *72*(1) (2016), 64-75.